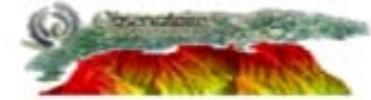


Seeing measurements for ground based solar astrometry

Rabah Ikhlef
and the Picard-Sol team



Outline of the presentation

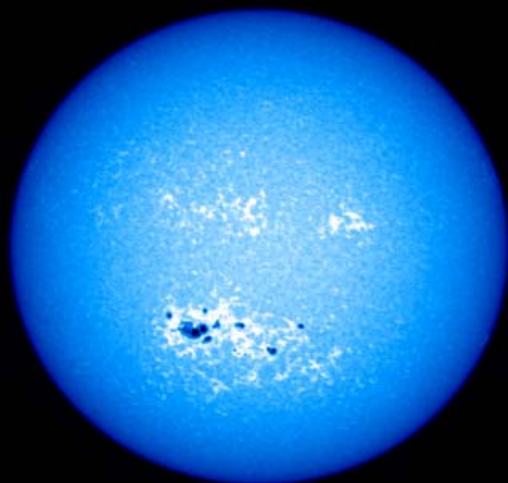
- Introduction
- Picard-Sol instruments
- Turbulence measurements methods overview
- Seeing estimation from full disk long exposure solar images
- Correction of radius measurements from seeing effects
- Conclusion

PICARD

Mission d'étude des relations entre la variabilité **solaire** et le **climat** de la Terre. Mieux comprendre les changements climatiques par une meilleure connaissance du Soleil.

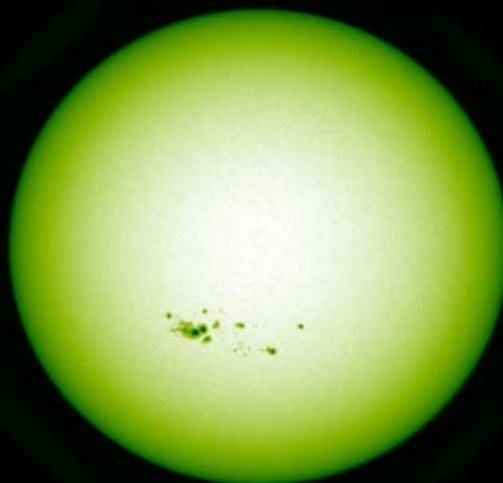


2012-07-11 06:56 UTC



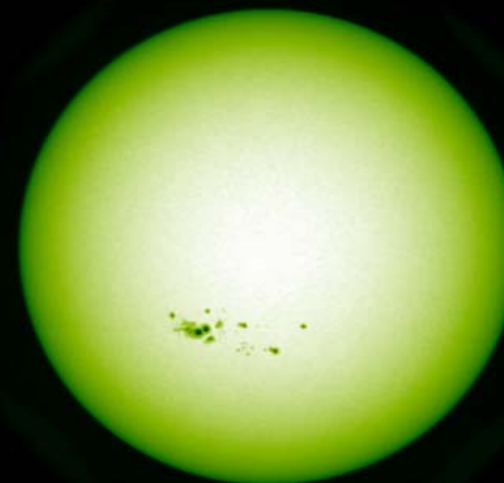
© Centre de Recherche Atmosphères - LATMOS - CNRS

2012-07-11 10:02 UTC



© Centre de Recherche Atmosphères - LATMOS - CNRS

2012-07-11 07:01 UTC



© Centre de Recherche Atmosphères - LATMOS - CNRS

2012-07-11 08:07 UTC



© Centre de Recherche Atmosphères - LATMOS - CNRS

2012-07-11 14:39 UTC

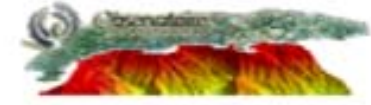


© Centre de Recherche Atmosphères - LATMOS - CNRS

2012-07-11 08:29 UTC



© Centre de Recherche Atmosphères - LATMOS - CNRS

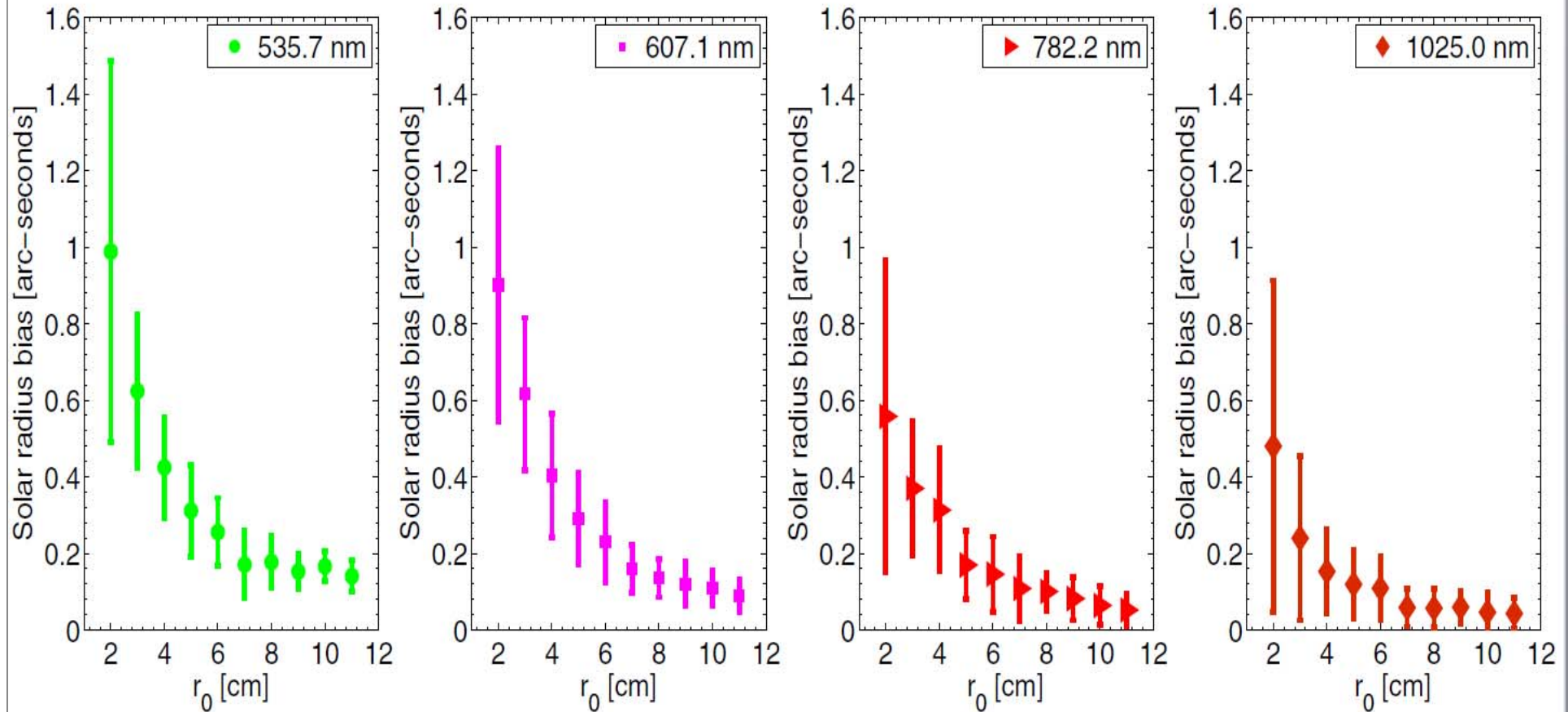


Daytime turbulence

- Optical turbulence affects strongly ground based observations.
- Variations in temperature \rightarrow fluctuations in the index of refraction of air $n \rightarrow$ turbulent wavefront.
- Daytime turbulence localised near the surface.
- Most of the dispersion in radius measurement is due to seeing.
- Importance of estimating the seeing and the characteristic time.
- Simulations of bias introduced by turbulence.



Simulation of the bias due to Fried parameter on SODISM2 measurements

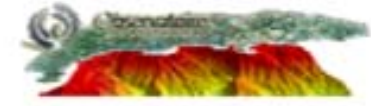


PICARD

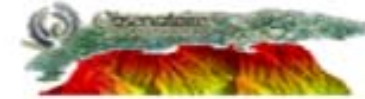
Mission d'étude des relations entre la variabilité **solaire** et le **climat** de la Terre. Mieux comprendre les changements climatiques par une meilleure connaissance du Soleil.



LATMOS



Daytime seeing estimation techniques



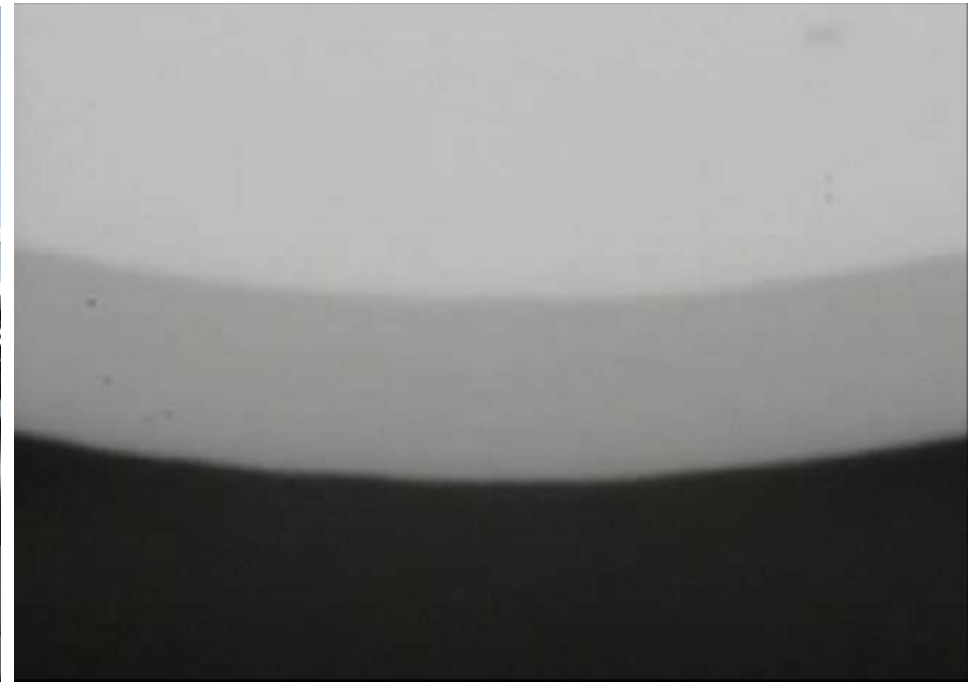
Main estimation techniques

- Solar Differential image Motion Monitor (S-DIMM)
- SODAR
- SHAdow BAnd Ranger (SHABAR): consisting of an array of solar scintillometers for the measurement of the atmospheric structure constant $C_n^2(h)$
- Shack-Hartmann of a solar adaptive optics system.
- MISOLFA: Angle-of-arrival fluctuations from solar limb images → spatial parameters (r_0 , $L_0(h)$, $C_n^2(h)$)

Intensity fluctuations in pupil plane → τ_0 , r_0 , L_0

- MTF of long exposure images: r_0

Solar DIMM

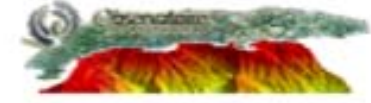


$$\sigma^2 = K_l \lambda^2 r_0^{-5/3} D^{-1/3}.$$

$$K_l = 0.364 \left(1 - 0.532 b^{-1/3} - 0.024 b^{-7/3} \right)$$

Beckers 2001

Özişik et al. 2004



Main estimation techniques

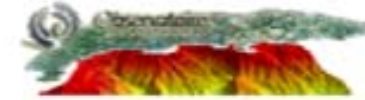
- Solar Differential image Motion Monitor (S-DIMM)
- SODAR
- SHAdow BAnd Ranger (SHABAR): consisting of an array of solar scintillometers for the measurement of the atmospheric structure constant $Cn^2(h)$
- Shack-Hartmann of a solar adaptive optics system.
- MISOLFA: Angle-of-arrival fluctuations from solar limb images → spatial parameters (r_0 , $L_0(h)$, $Cn^2(h)$)

Intensity fluctuations in pupil plane → τ_0 , r_0 , L_0

- MTF of long exposure images: r_0



SODAR (SO^Nic Detection And Ranging) is a wind profiler to measure the scattering of sound waves by atmospheric turbulence.



Main estimation techniques

- Solar Differential image Motion Monitor (S-DIMM)
- SODAR
- SHAdow BAnd Ranger (SHABAR): consisting of an array of solar scintillometers for the measurement of the atmospheric structure constant $C_n^2(h)$
- Shack-Hartmann of a solar adaptive optics system.
- MISOLFA: Angle-of-arrival fluctuations from solar limb images → spatial parameters (r_0 , $L_0(h)$, $C_n^2(h)$)

Intensity fluctuations in pupil plane → τ_0 , r_0 , L_0

- MTF of long exposure images: r_0

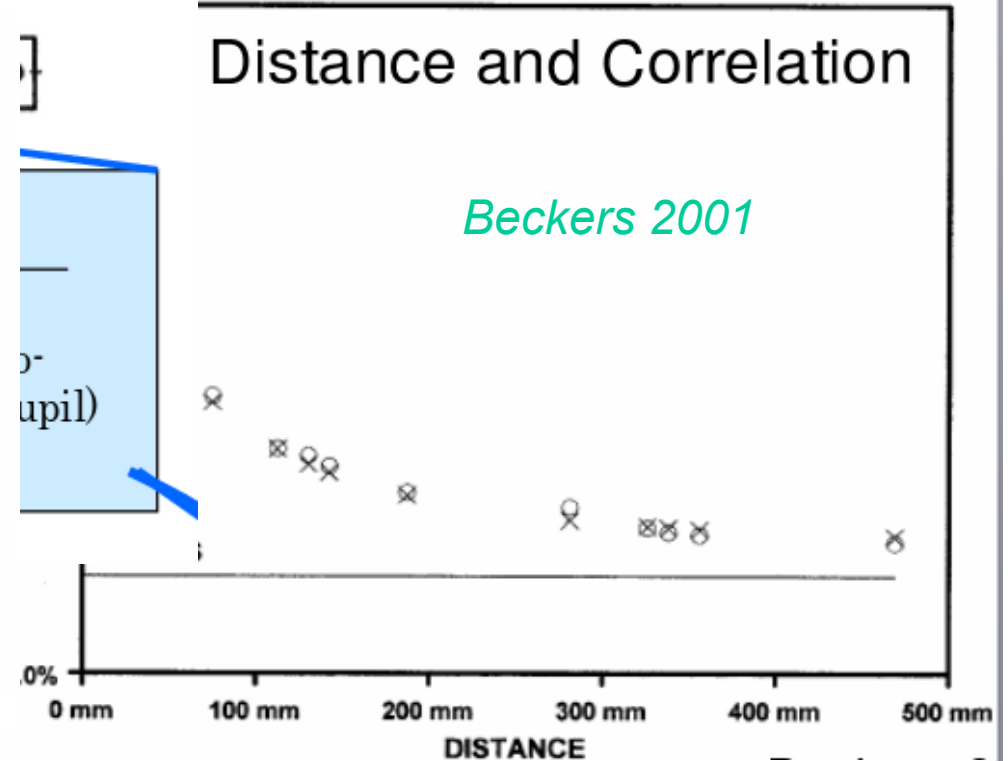
SHABAR Array

SHABAR array l ~ 50cm



S-DIMM Apertures
d ~ 23cm

Distance and Correlation



σ_I^2 stars: $1 \sim 10^{-3}$ the Sun: $10^{-6} \sim 10^{-8}$

– Fried parameter and scintillation: anti-correlation

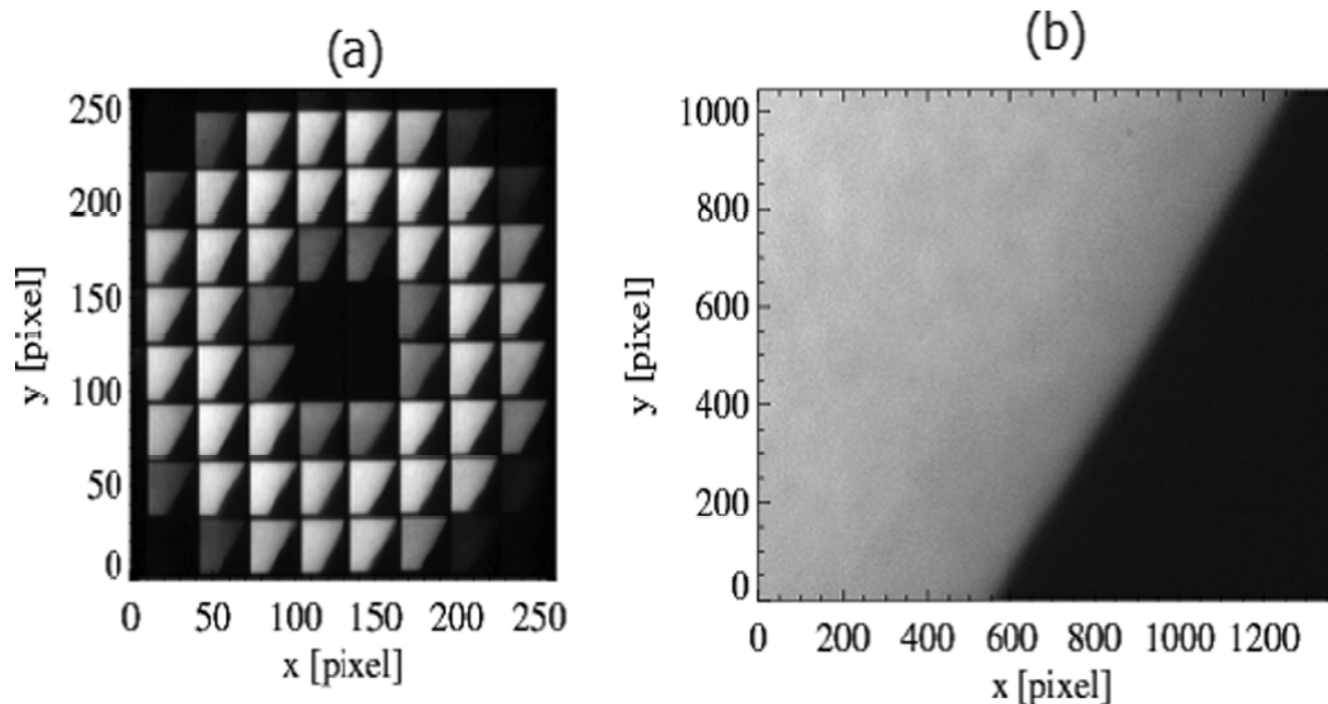
Main estimation techniques

- Solar Differential image Motion Monitor (S-DIMM)
- SODAR
- SHAdow BAnd Ranger (SHABAR): consisting of an array of solar scintillometers for the measurement of the atmospheric structure constant $C_n^2(h)$
- Shack-Hartmann of a solar adaptive optics system.
- MISOLFA: Angle-of-arrival fluctuations from solar limb images → spatial parameters (r_0 , $L_0(h)$, $C_n^2(h)$)

Intensity fluctuations in pupil plane → τ_0 , r_0 , L_0

- MTF of long exposure images: r_0

Shack-Hartmann



Kawate 2011

- Use of a solar adaptive optics part to measure seeing
- Each paire of subapertures is regarded as a DIMM
- r_0 is estimated from differential image motions
- Method of Sarazin & Roddier 1990

Main estimation techniques

- Solar Differential image Motion Monitor (S-DIMM)
- SODAR
- SHAdow BAnd Ranger (SHABAR): consisting of an array of solar scintillometers for the measurement of the atmospheric structure constant $Cn^2(h)$
- Shack-Hartmann of a solar adaptive optics system.
- MISOLFA: Angle-of-arrival fluctuations from solar limb images → spatial parameters (r_0 , $L_0(h)$, $Cn^2(h)$)

Intensity fluctuations in pupil plane → τ_0 , r_0 , L_0

- MTF of long exposure images: r_0

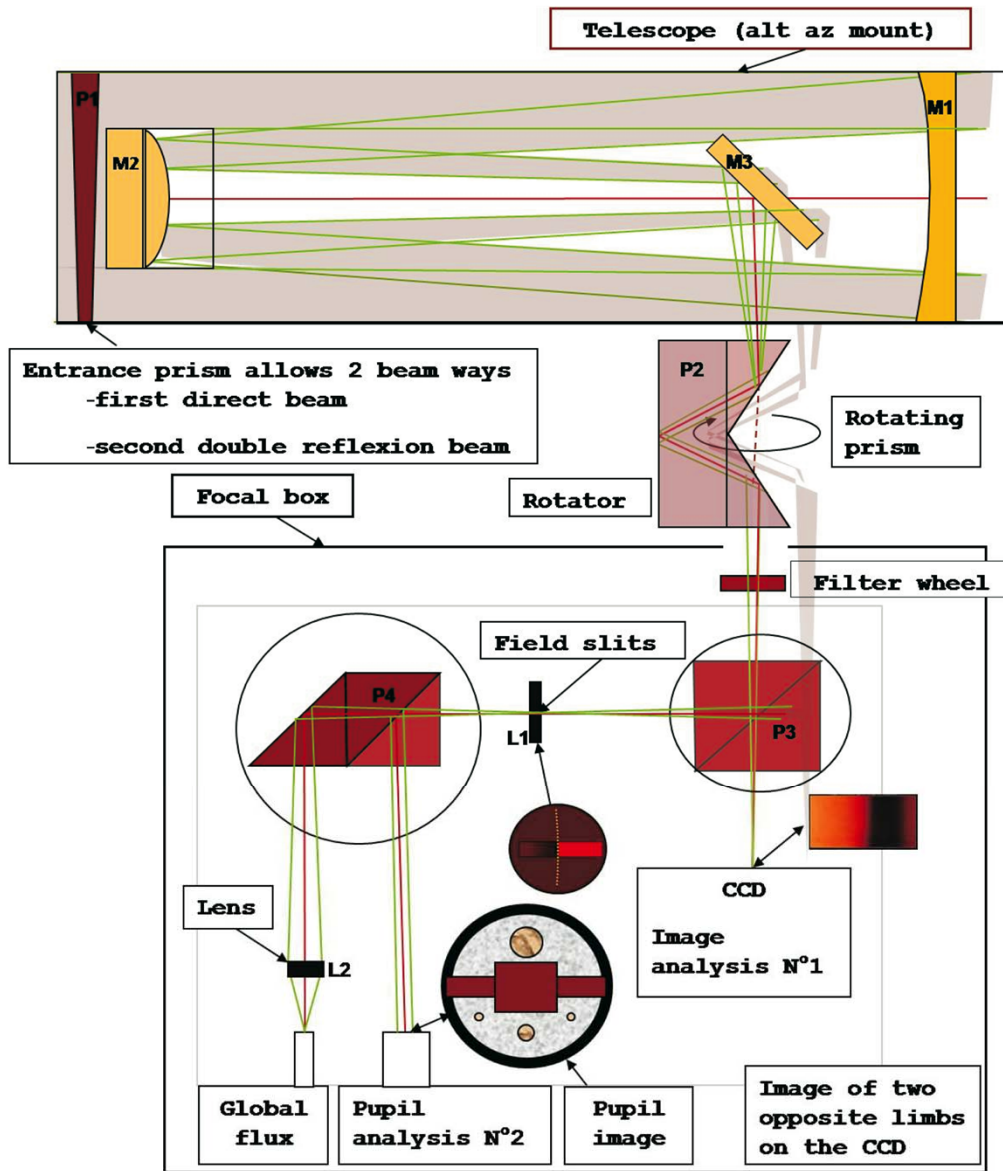
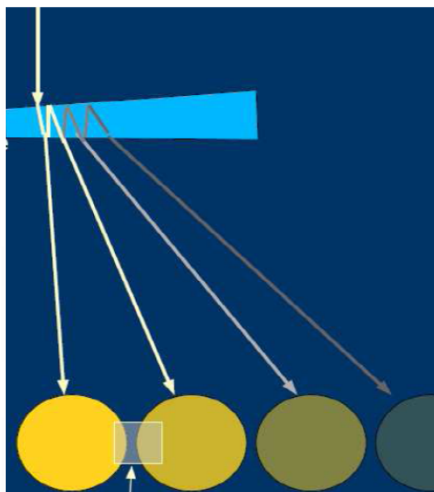
Picard-Sol instruments



SODISM II

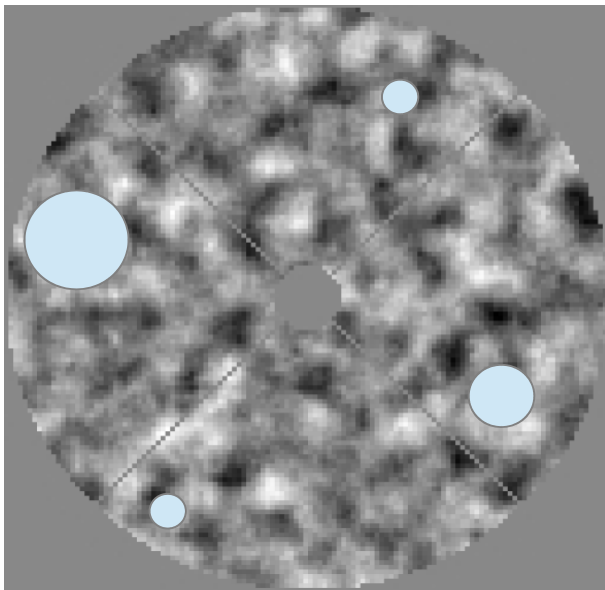
MISOLFA

MISOLFA



Data processing

Pupil plane



Fluctuation d'intensité voie pupille corrigées de la valeur moyenne

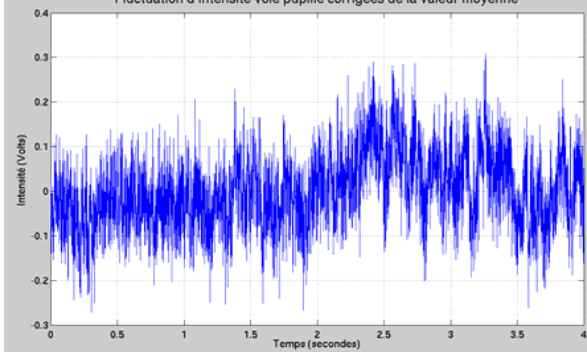
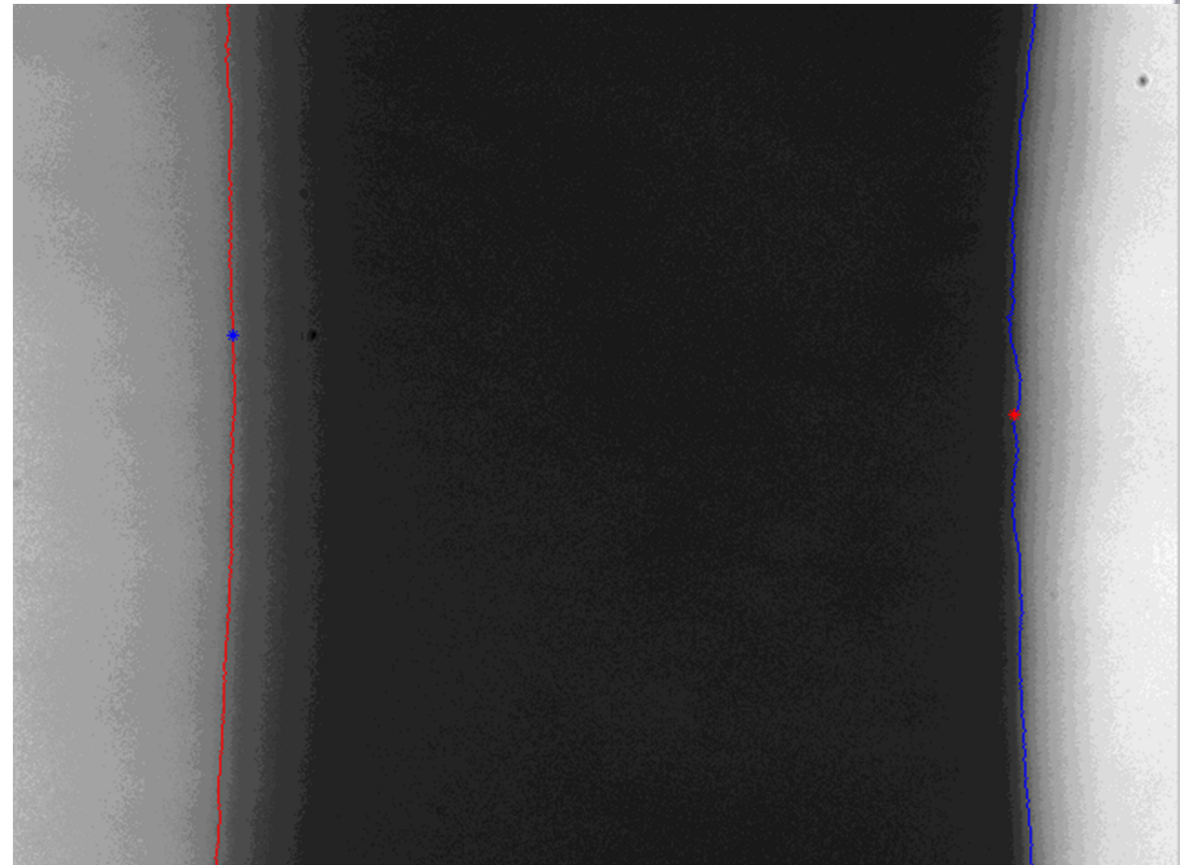
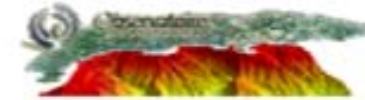
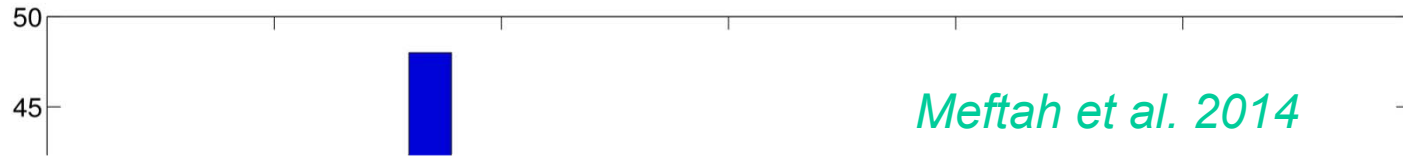


Image plane

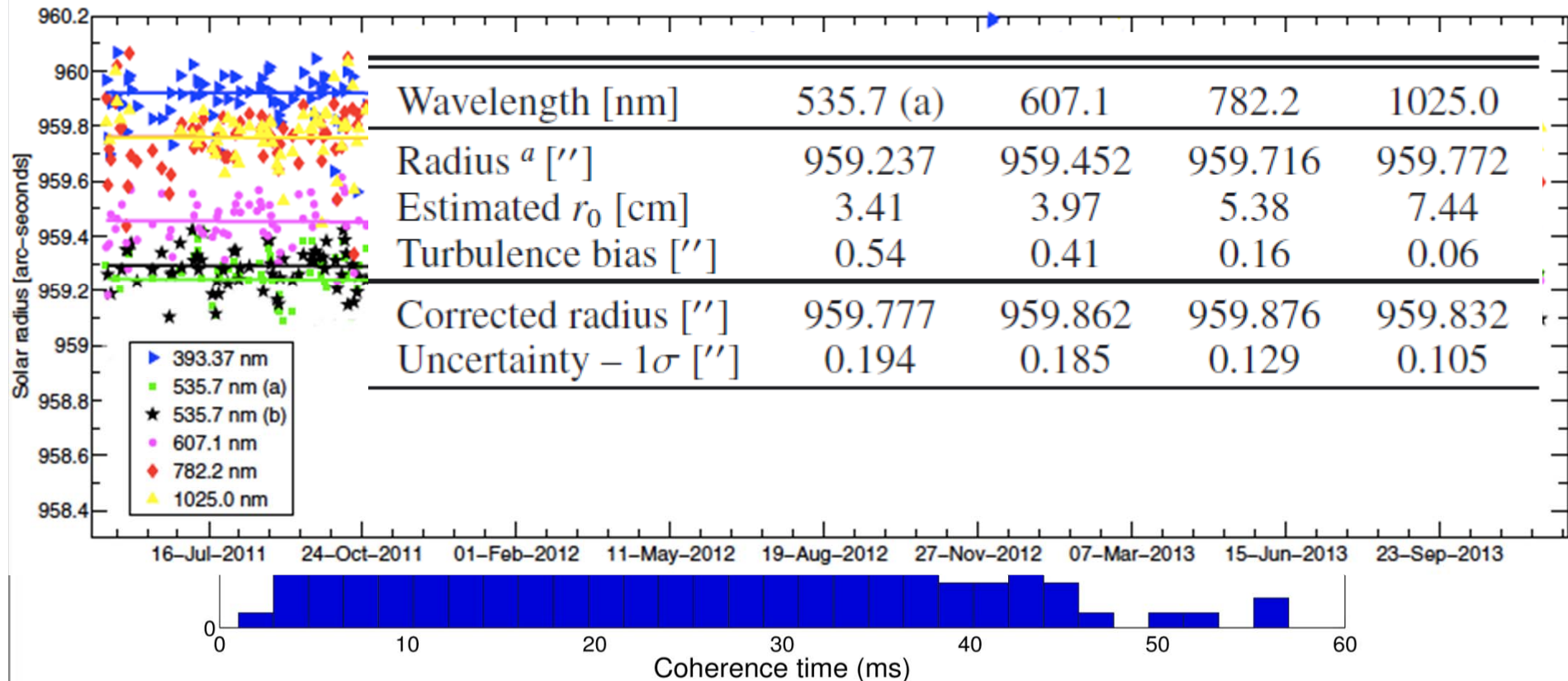




Some results from MISOLFA: image and pupil plane

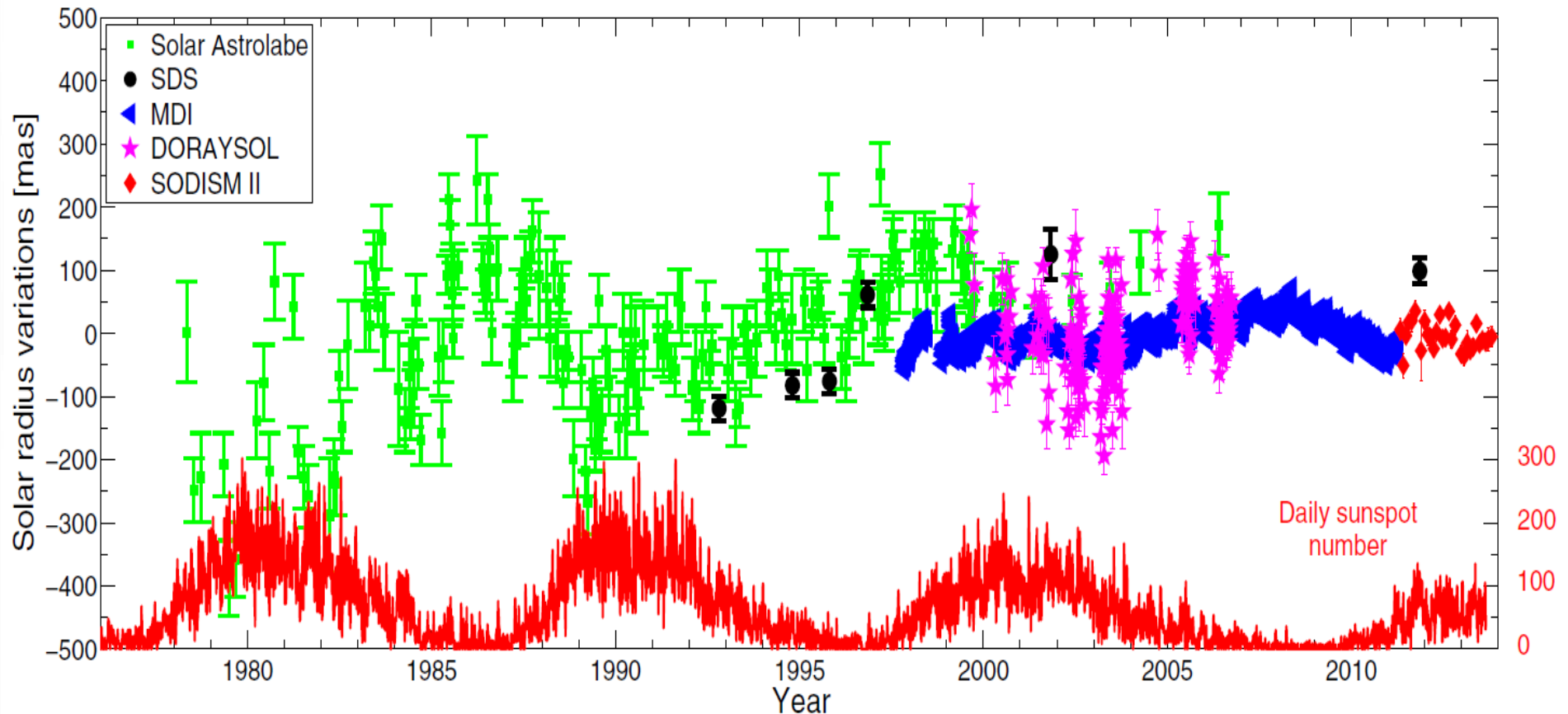


Meftah et al. 2014



Picard-Sol results after seeing effect correction

A&A 569, A60 (2014) *Meftah et al. 2014*

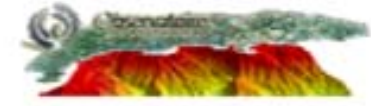


PICARD

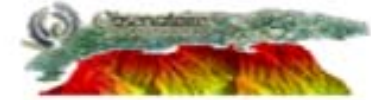
Mission d'étude des relations entre la
variabilité **solaire** et le **climat** de la Terre.
Mieux comprendre les changements
climatiques par une meilleure
connaissance du Soleil.



LATMOS



Estimation of r_0 using long exposure images MTF



Method

Bell, Hill and Harvey 1999

- Recorded image of the Sun:

$$o(\lambda, x, y) = i(\lambda, x, y) \otimes \psi(\lambda, x, y) + \cancel{n(\lambda, x, y)}$$

- In the Fourier domain (circularly symmetric): Hankel transform

$$O(q) = I(q)\Psi(q)$$

- The modulation transfer function can be expressed for long exposure images as :

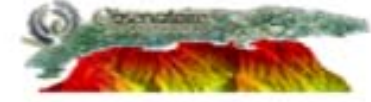
$$\Psi(q) = e^{-3.44(\lambda q/r_0)^{5/3}}$$

- In the general case:

$$\Psi(q) \approx e^{-3.35(\lambda q/r_0)^n}$$

- Introducing a diffusion term as a Lorentzian in MTF equation gives:

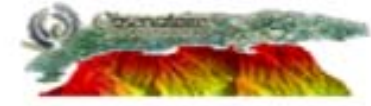
$$\Psi(q) = (1 - \epsilon)e^{-3.35(\lambda q/r_0)^n} + \epsilon e^{-Aq}$$



MTF estimation from full disk images

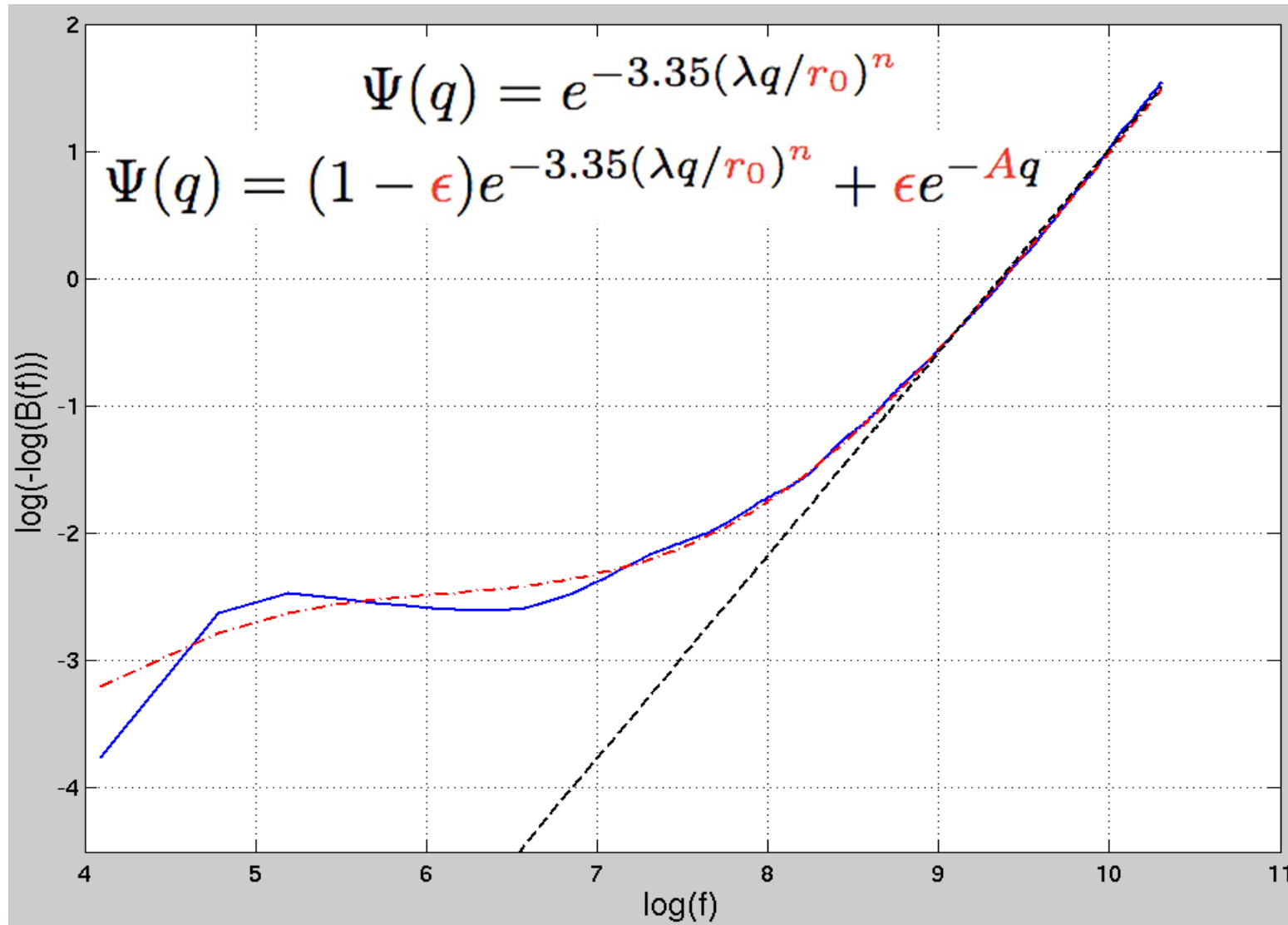
Toner & Jefferies 1993

- Accurate determination of the full disk geometry, fit by an ellipse.
- Generation of the radial intensity profile (median in successive annuli) rejecting pixels contaminated by activity.
- Application of the Hankel transform.
- Determination of the positions of the zeros crossings the transformed data.
- Least square minimization to determine limb darkening coefficients, ellipse parameters and mean radius.
- Estimation of the MTF for the image.

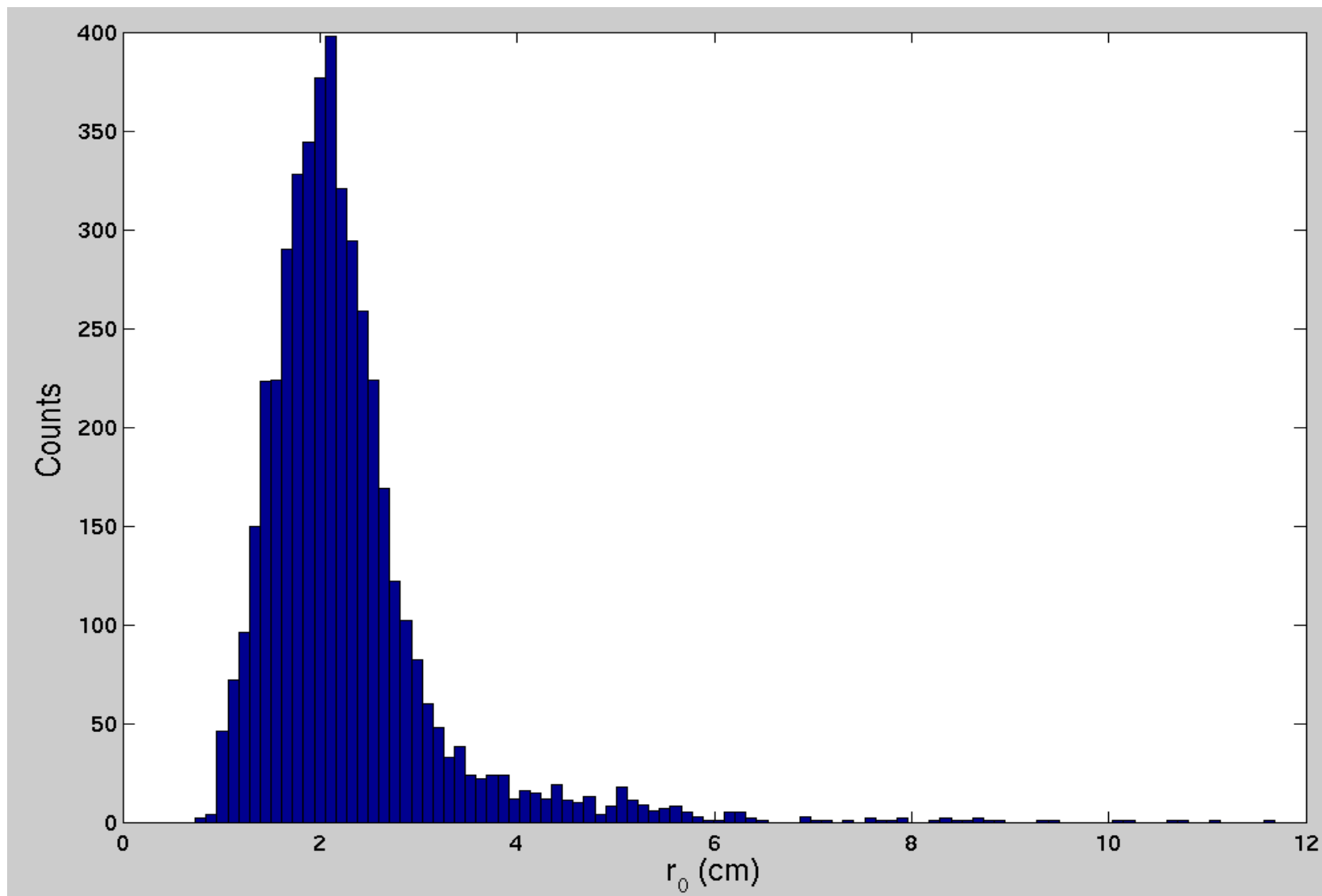


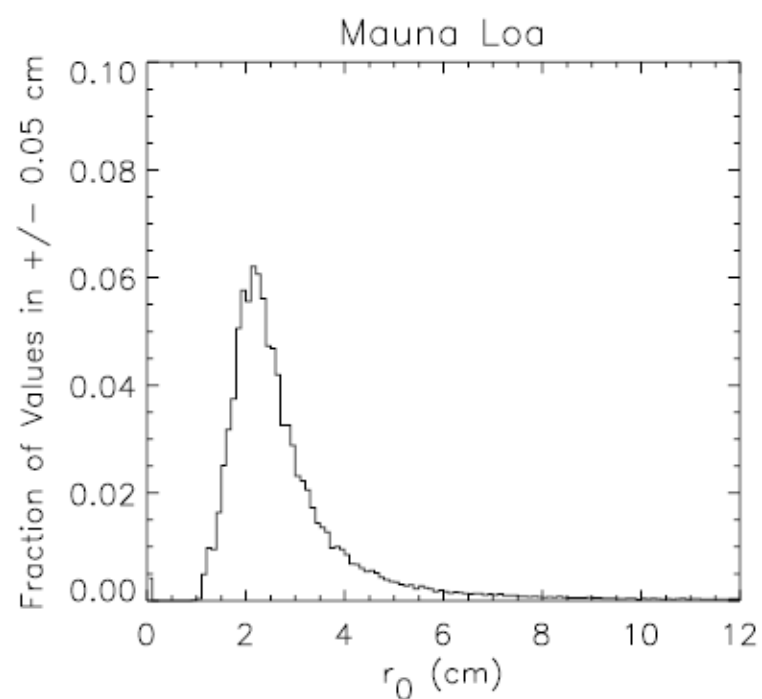
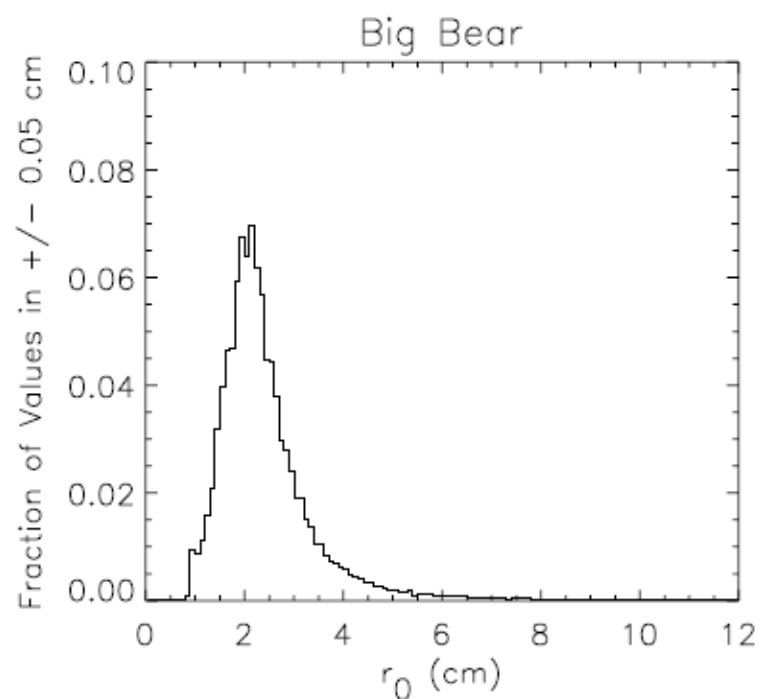
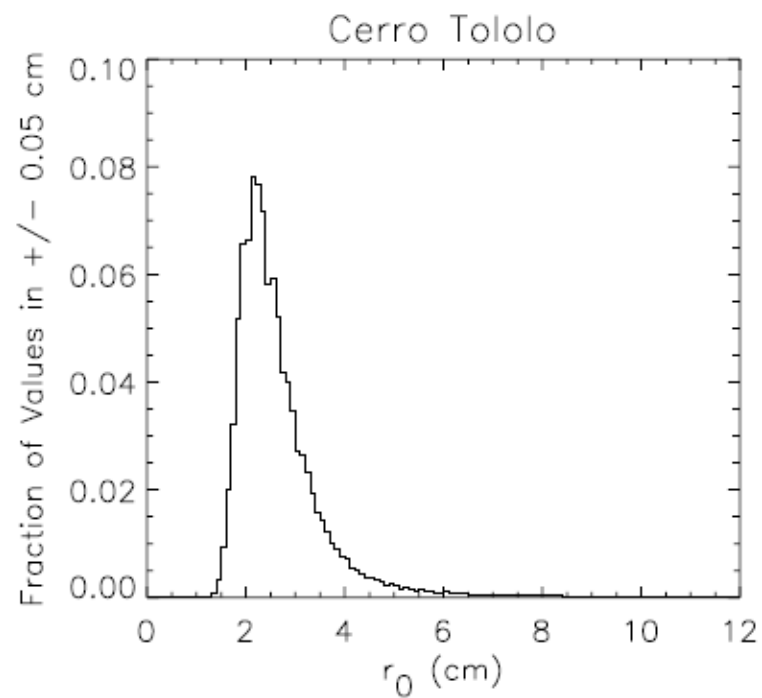
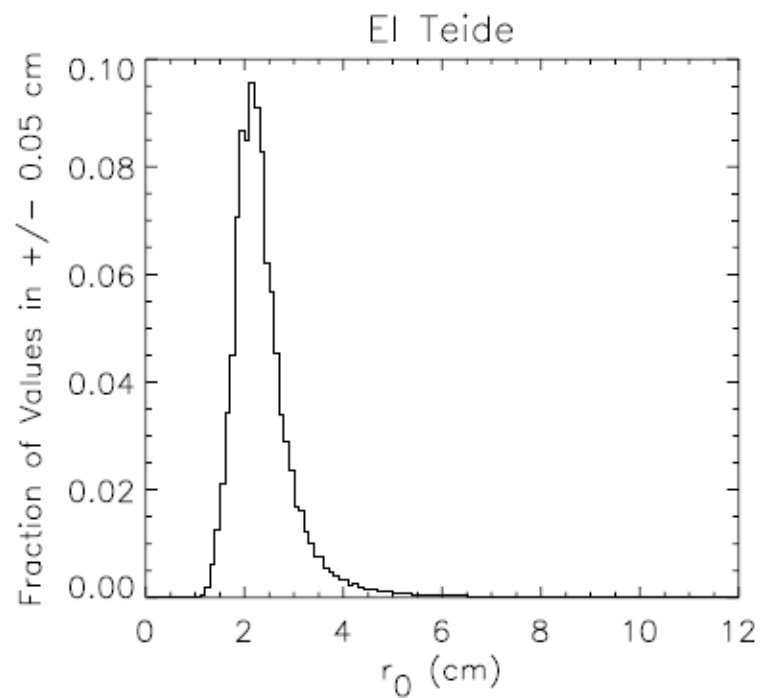
MTF estimation from SODISM2 images

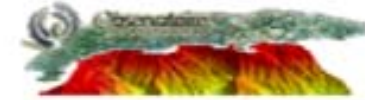
-
-



Histogram @ 607nm







Conclusions and perspectives

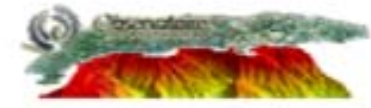
- Simple parametrization allows us to estimate a mean value of Fried parameter together with the image MTF and limb darkening coefficients for each SODISM2 images.
- MISOLFA also provides estimates to the instantaneous Fried parameter values.
- Need to be calibrated with other instruments (S-DIMM, PBL).
- Knowledge of seeing allow image restoration and correction of measured radii.
- MISOLFA provides estimates of turbulence coherence time -> Reconstruction the optical turbulence part of the long exposure MTF and help to separate the different contributions of the global MTF.
- Scattering effect appears to be negligible in comparison to seeing..

PICARD

Mission d'étude des relations entre la
variabilité **solaire** et le **climat** de la Terre.
Mieux comprendre les changements
climatiques par une meilleure
connaissance du Soleil.



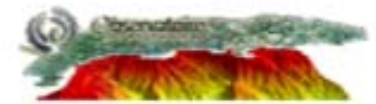
LATMOS



Thank you !

PICARD

Mission d'étude des relations entre la
variabilité **solaire** et le **climat** de la Terre.
Mieux comprendre les changements
climatiques par une meilleure
connaissance du Soleil.

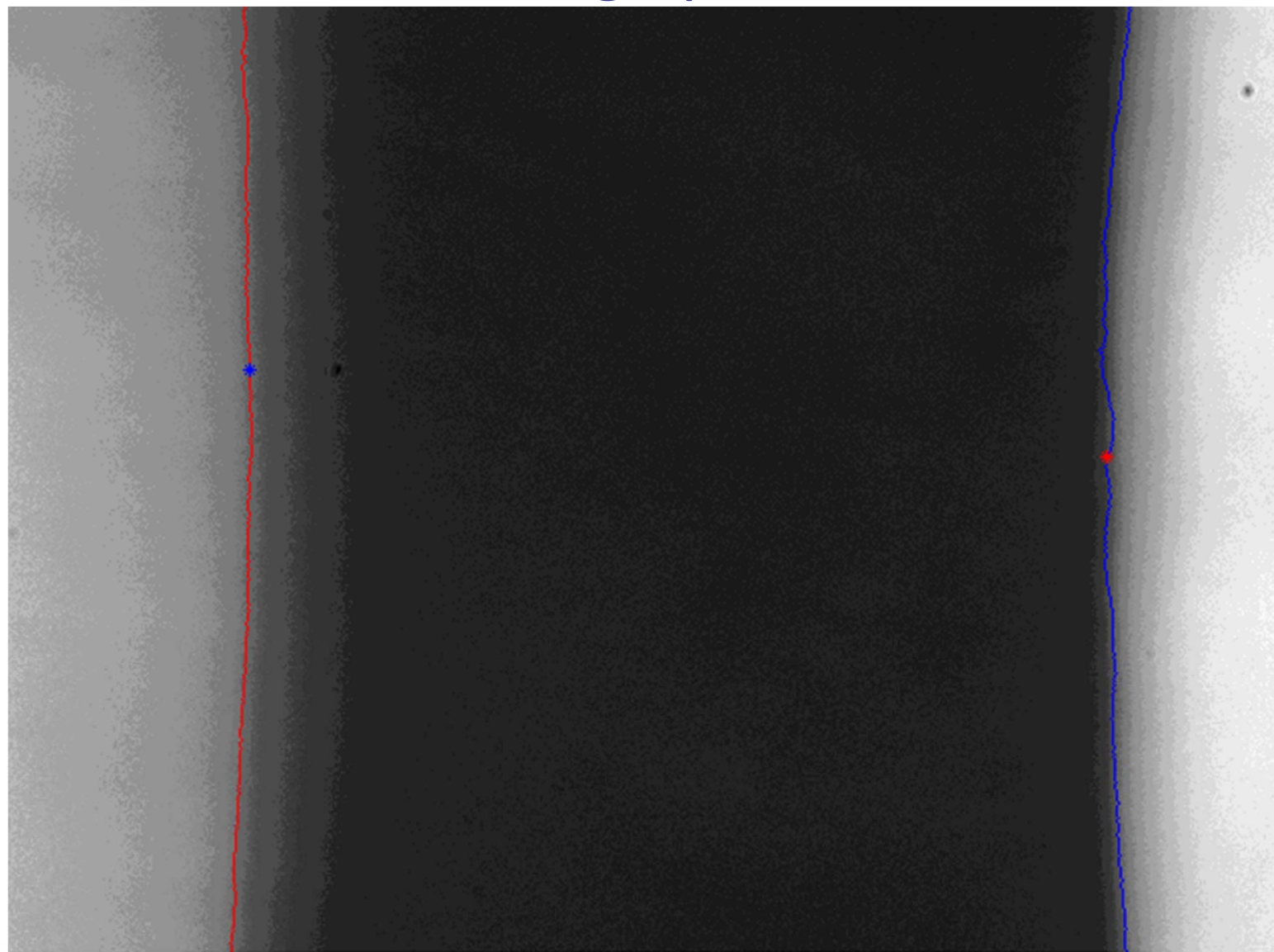


PICARD

Mission d'étude des relations entre la variabilité **solaire** et le **climat** de la Terre. Mieux comprendre les changements climatiques par une meilleure connaissance du Soleil.



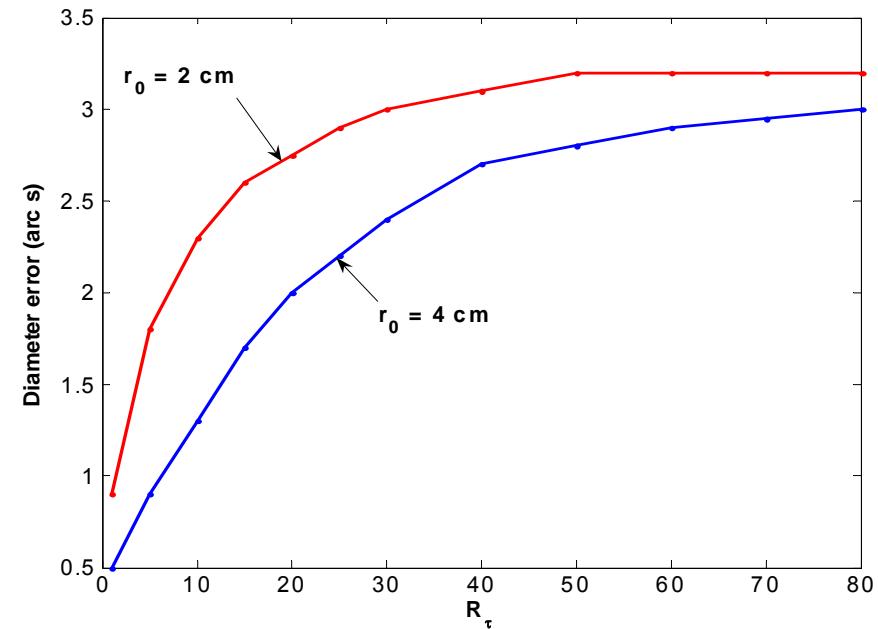
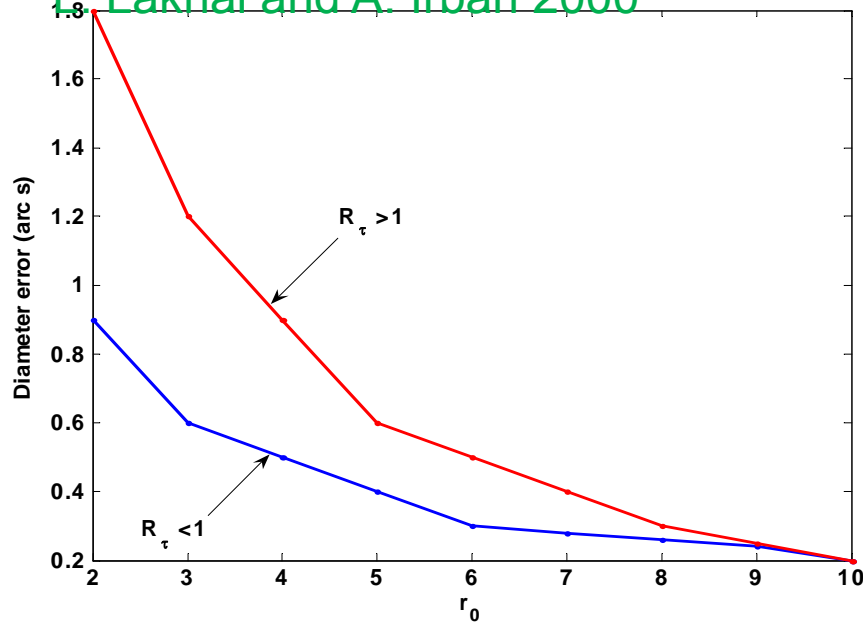
Image plane



Seeing effect: Why MISOLFA ?

Atmospheric turbulence effects on solar diameter measurements : validation of numerical simulation using data recorded at Calern Observatory (with Doraysol)

L. Lakhali and A. Irbah 2000



Estimated errors on diameter estimates as a function of the Fried's parameter r_0 for two values of R_τ (ratio between the exposure time and the correlation time) (left) and as a function of R_τ for two values of r_0 (right)

Irbah et al., Solar Physics, 1994 Lakhali, Irbah et al., A&A, 1999

➤ Atmospheric Structure constant $C_n^2(h)$

➤ Fried's parameter r_0 is the diameter of the coherence zone of the degraded wave-front. It corresponds also to the image resolution obtained with the telescope of diameter r_0 placed outside the atmosphere.

$$r_0 = \left[16.7 \lambda^{-2} \int_0^{+\infty} dh C_n^2(h) \right]^{-\frac{3}{5}}$$

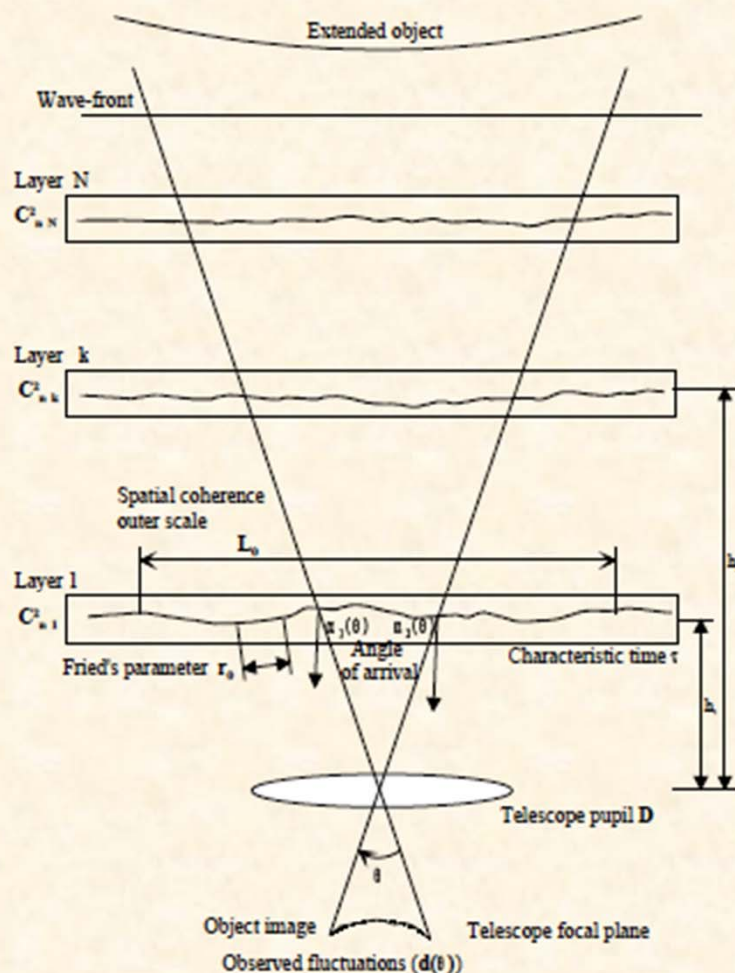
➤ The spatial coherence outer scale L_0 defines the maximal size of wave-front perturbations remaining coherent. It traduces of low frequency evolution of the wave-front.

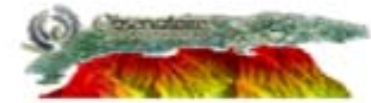
$$L_0 = \left[\frac{\int_0^{+\infty} dh L_0^{\frac{1}{3}} C_n^2(h)}{\int_0^{+\infty} dh C_n^2(h)} \right]^3$$

➤ Isoplanatic patch θ_0 is the angle where AA or speckles remain correlated.

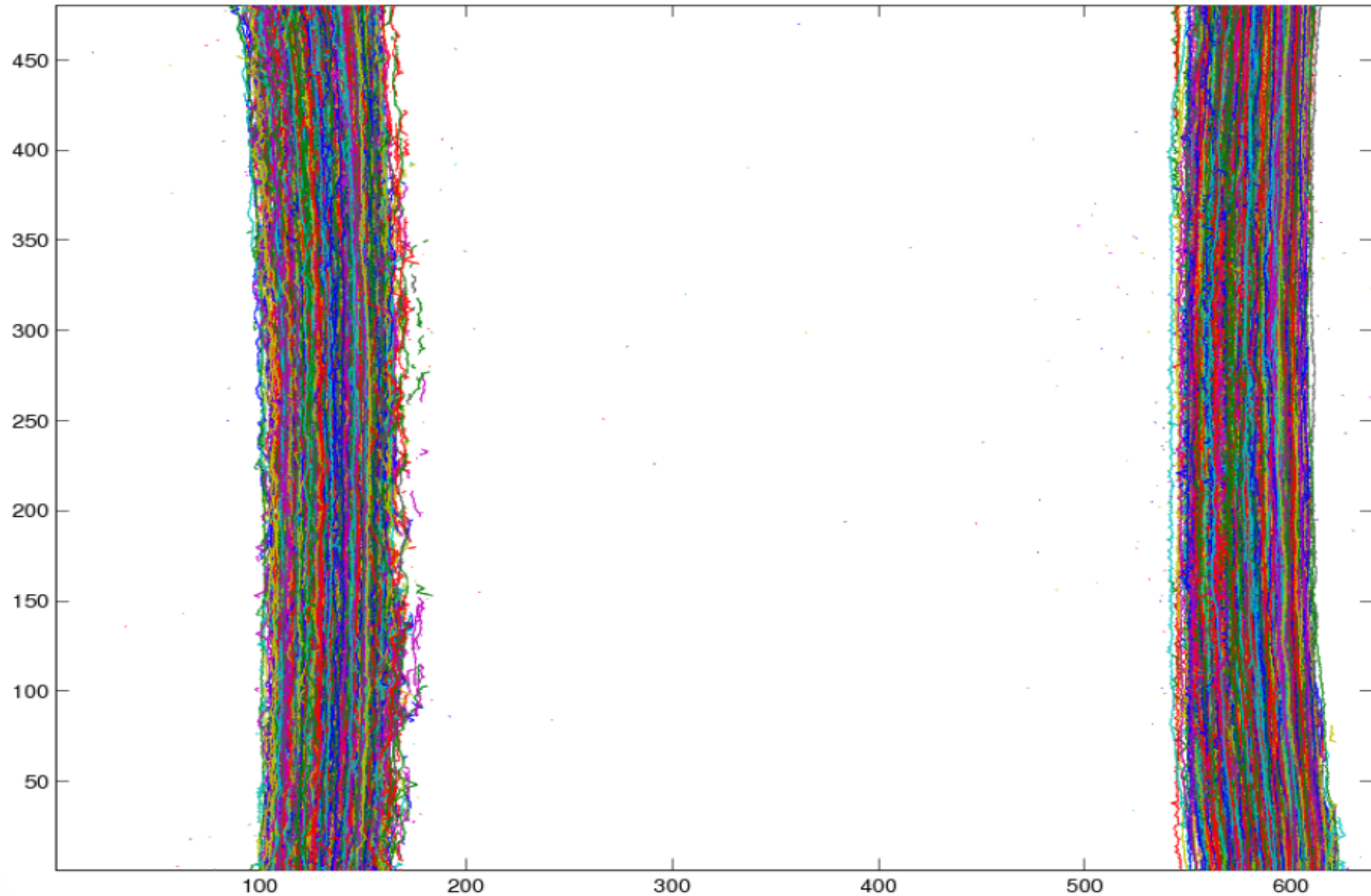
➤ Correlation time τ_0 is the time where the atmosphere may be considered as frizzed for the considered structures (AA, speckles). They keep their coherence

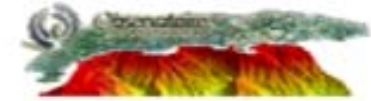
Multi-layers atmosphere with Von Karman turbulence model





Edges detection





Processing steps

- Image cleaning by wavelet denoising (sunspots)
- Solar edges extraction
- Angle-of-arrival fluctuations structure function

$$d_{\alpha_{\perp}Exp}(\theta) = \frac{1}{N} \sum_{i=1}^N \frac{1}{\theta_m - \theta} \sum_{k=1}^{\theta_m - \theta} [\alpha_{\perp}(k) - \alpha_{\perp}(k + \theta)]^2$$

- Non linear curve fitting assuming Von Karman model (Levenberg-Marquadt)

$$C_{\alpha}(\theta) = 0.0716\lambda^2 r_0^{-\frac{5}{3}} \int_0^{+\infty} df f^3 \left(f^2 + \frac{1}{L_0^2}\right)^{-\frac{11}{6}} [J_0(2\pi f\theta h) + J_2(2\pi f\theta h)] \left[\frac{2J_1(\pi Df)}{\pi Df}\right]^2$$

$$D_{\alpha}(\theta) = 2[C_{\alpha}(0) - C_{\alpha}(\theta)]$$

Examples

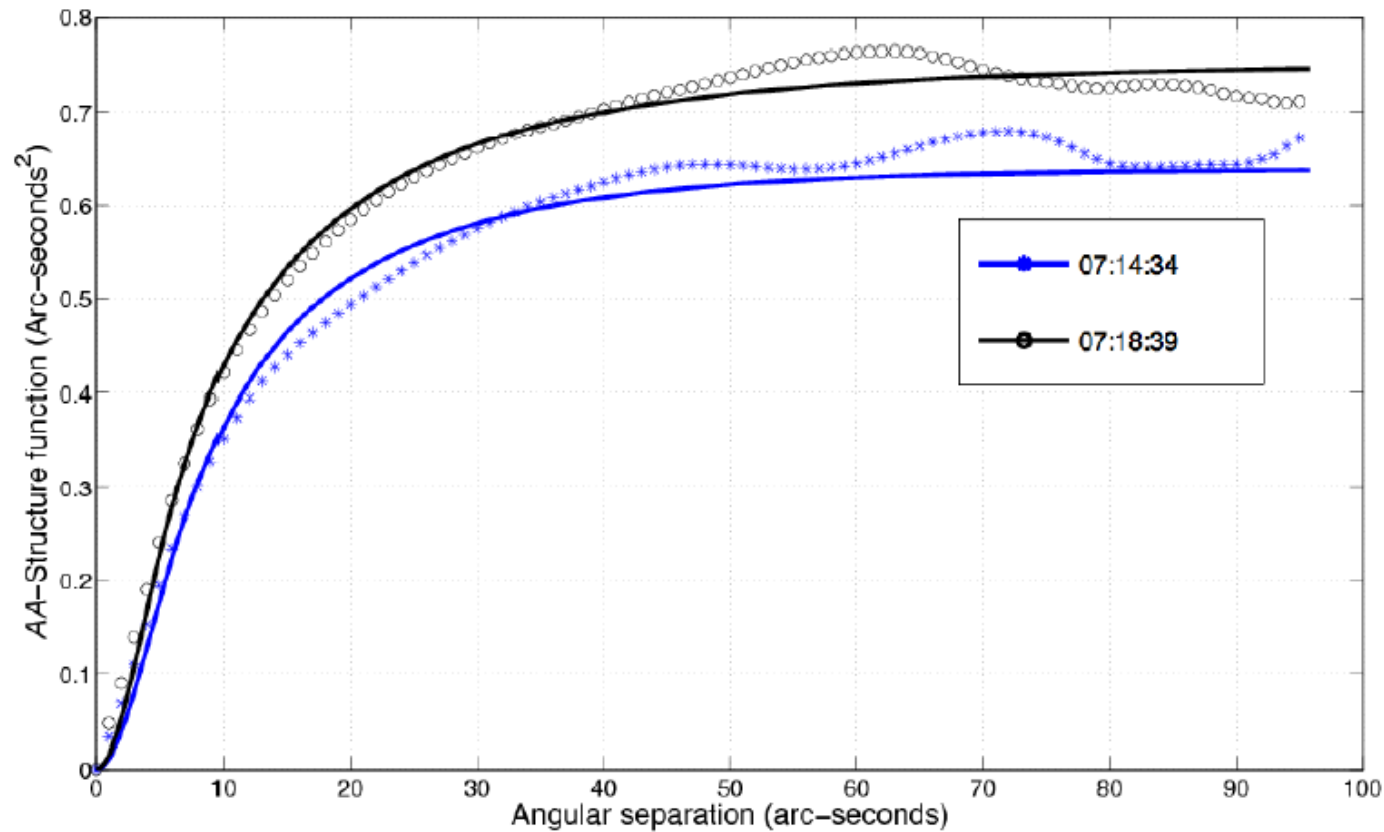
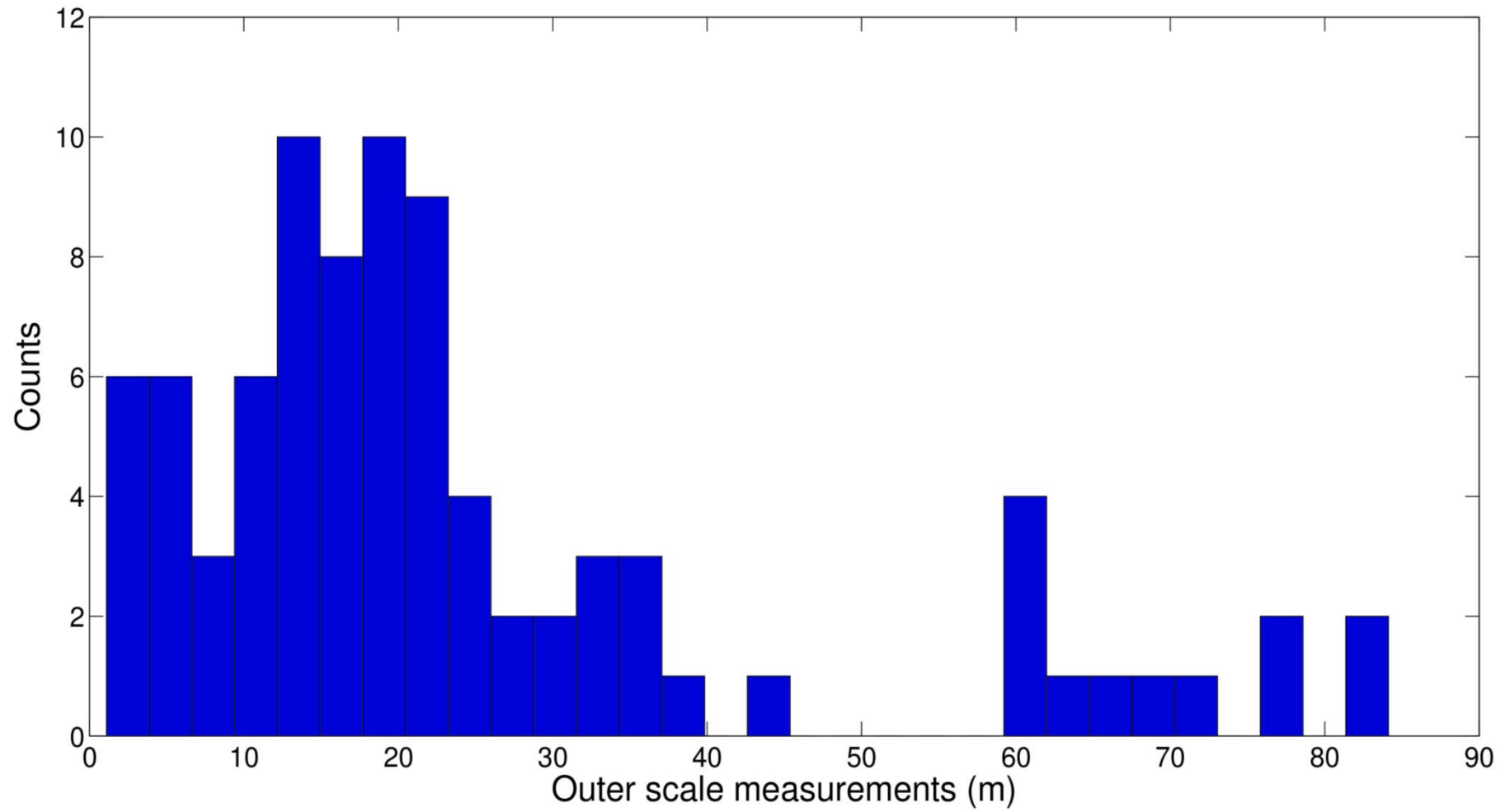
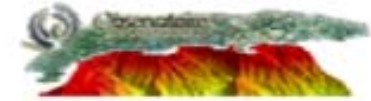
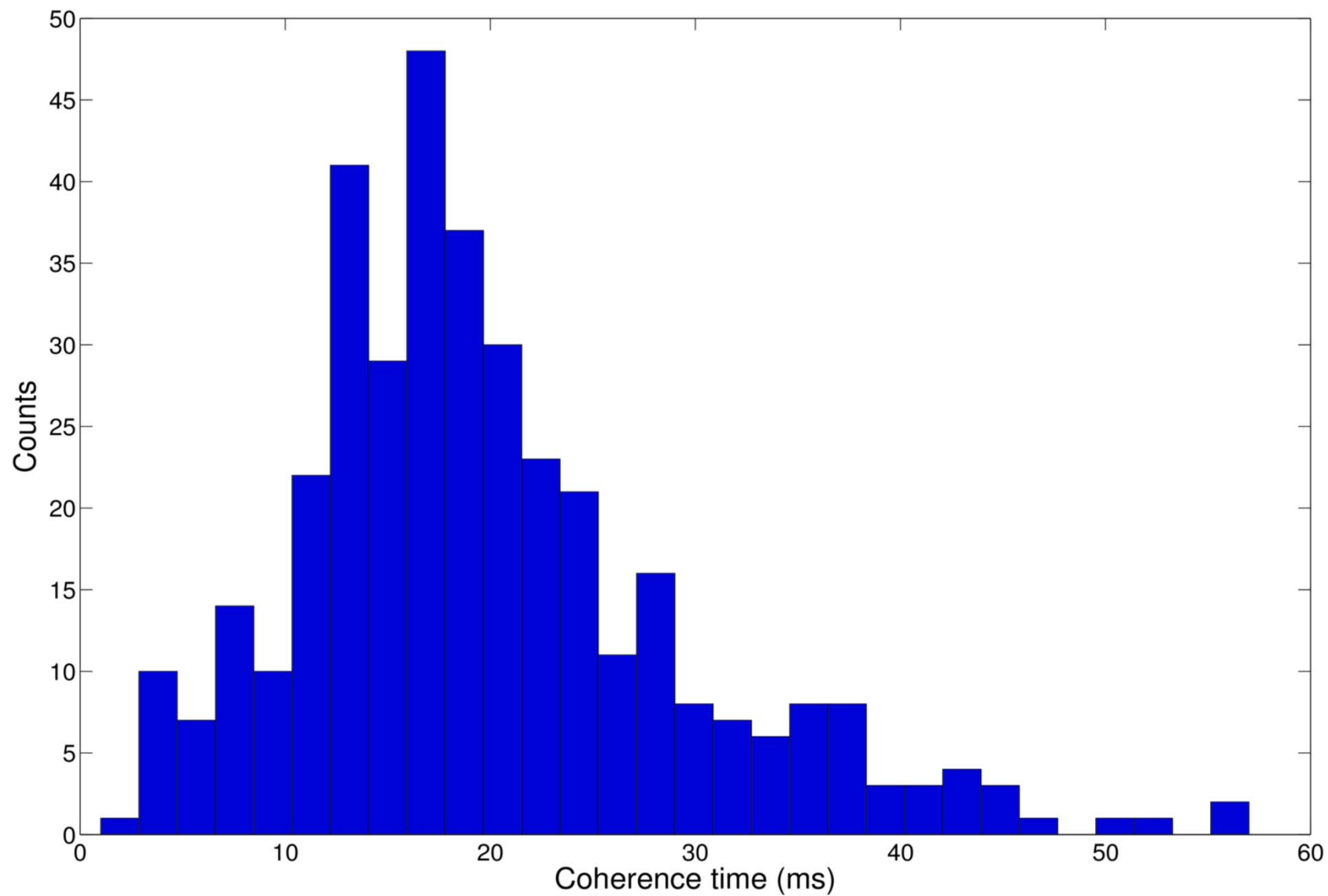


Figure 7. Experimental structure functions obtained on September 30th 2013. The non linear curve fitting (solid lines) allowed to extract spatial parameters. Values obtained are $h = 9152m$, $r_0 = 5.02cm$ and $\mathcal{L}_0 = 10.35m$ for the first curve (07:14:34) and $h = 9463m$, $r_0 = 4.56cm$ and $\mathcal{L}_0 = 9.66m$ for the second one.



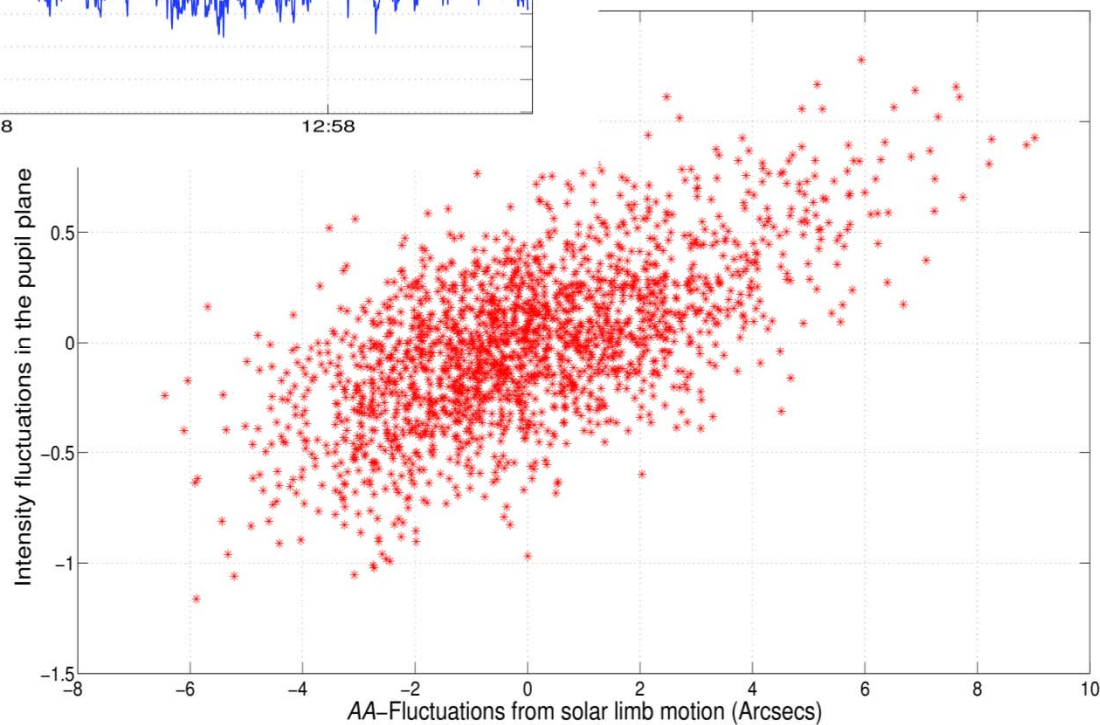
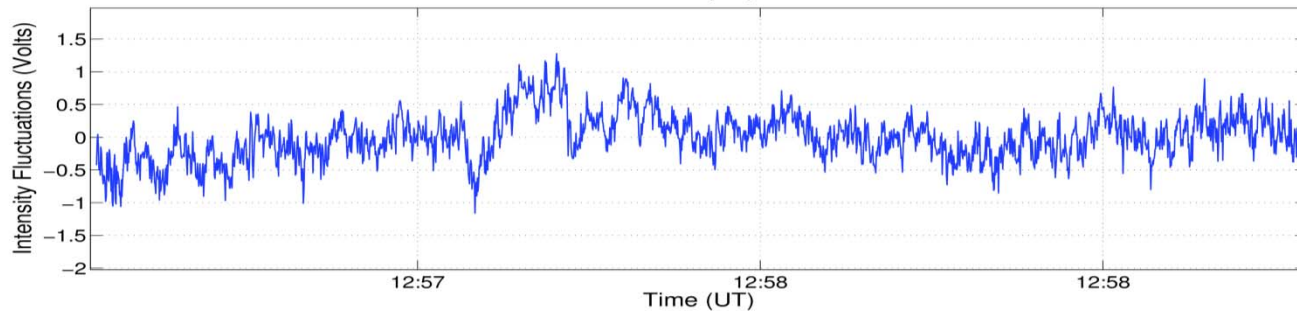
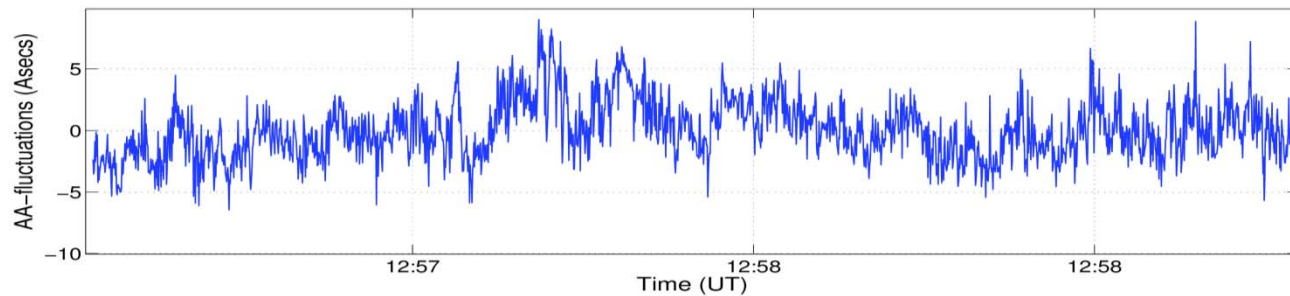


Pupil plane results



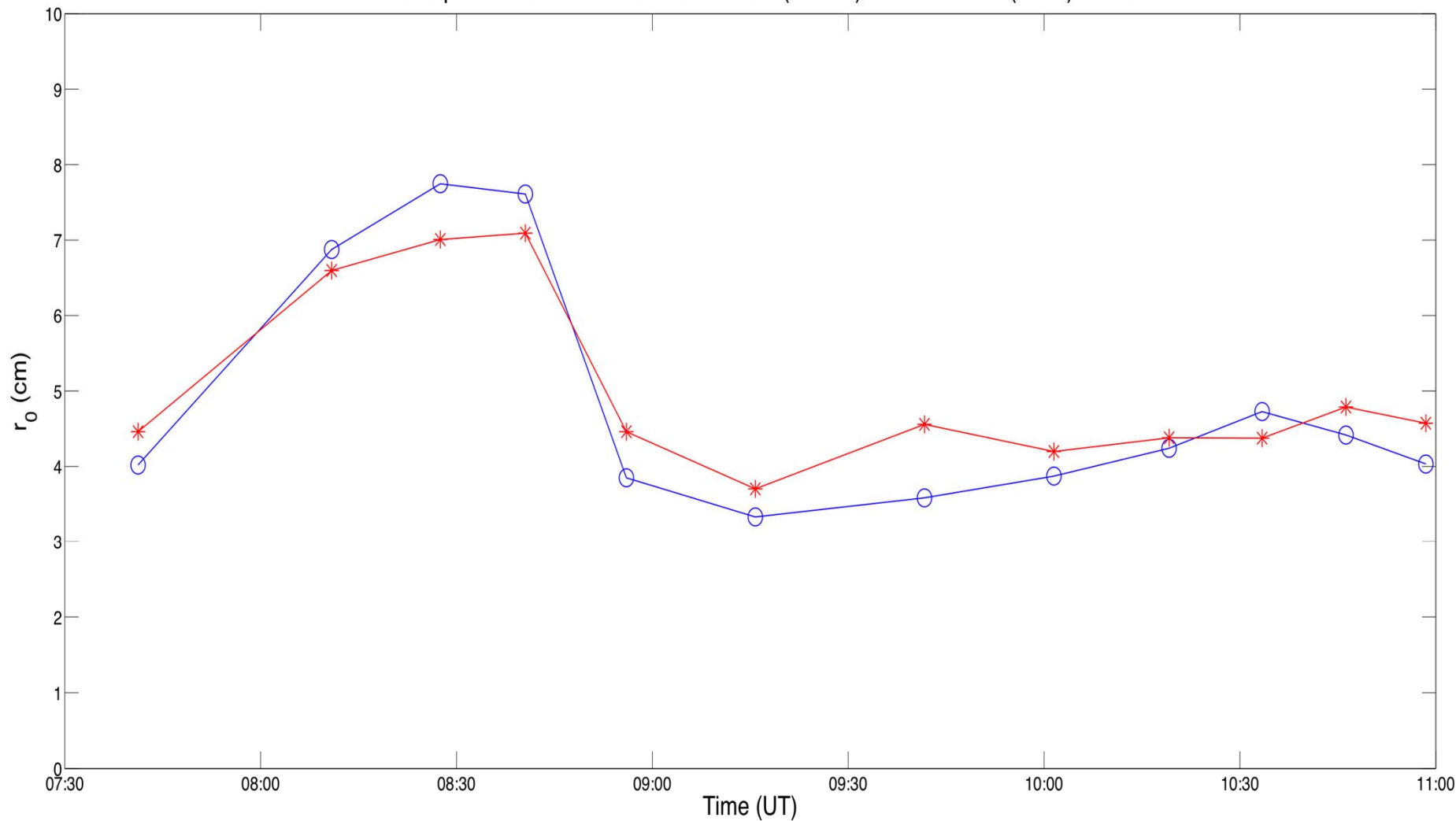


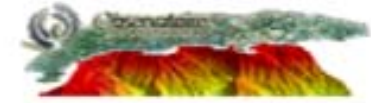
Calibration





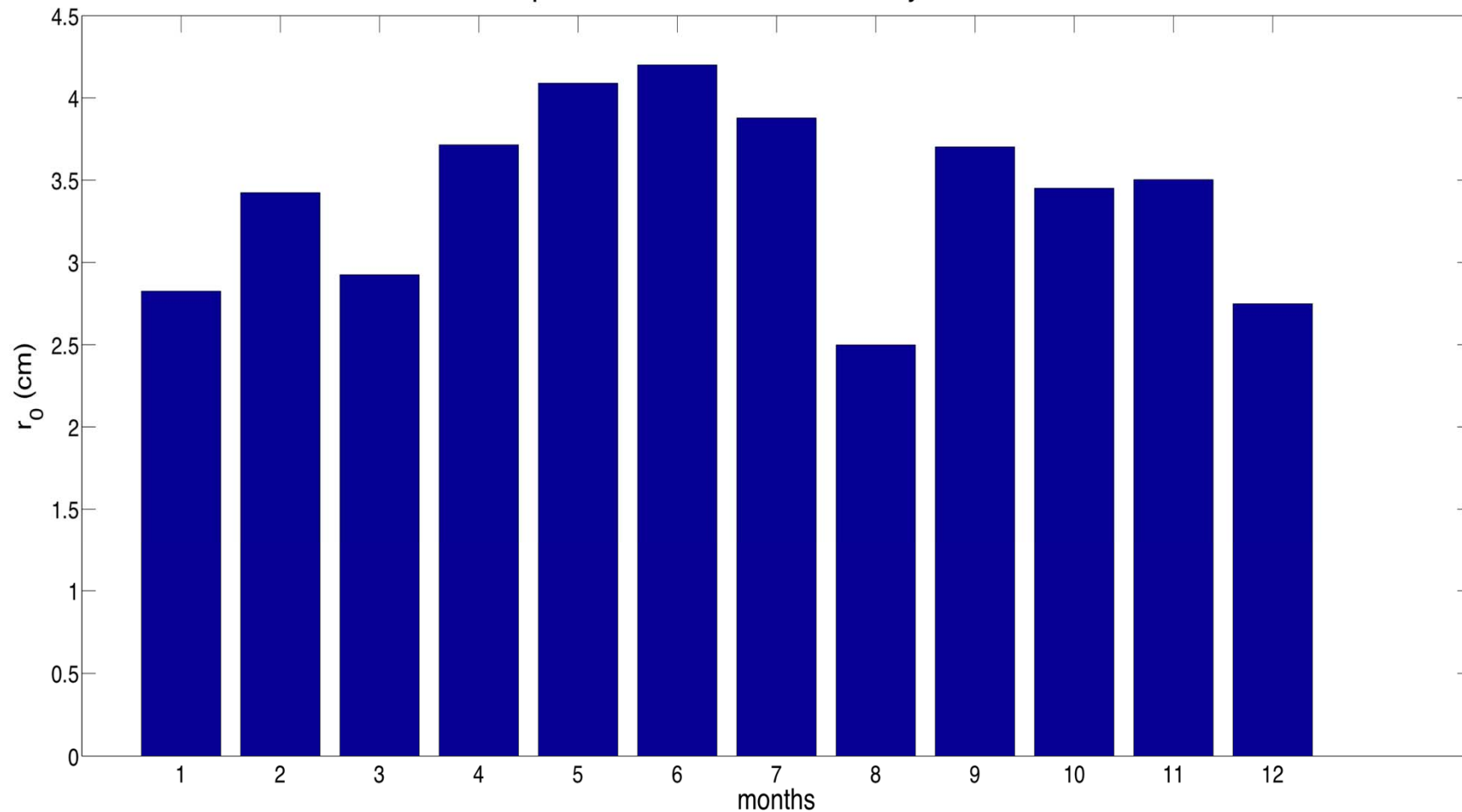
Fried's parameter estimation from direct (circles) and reflected (stars) limbs





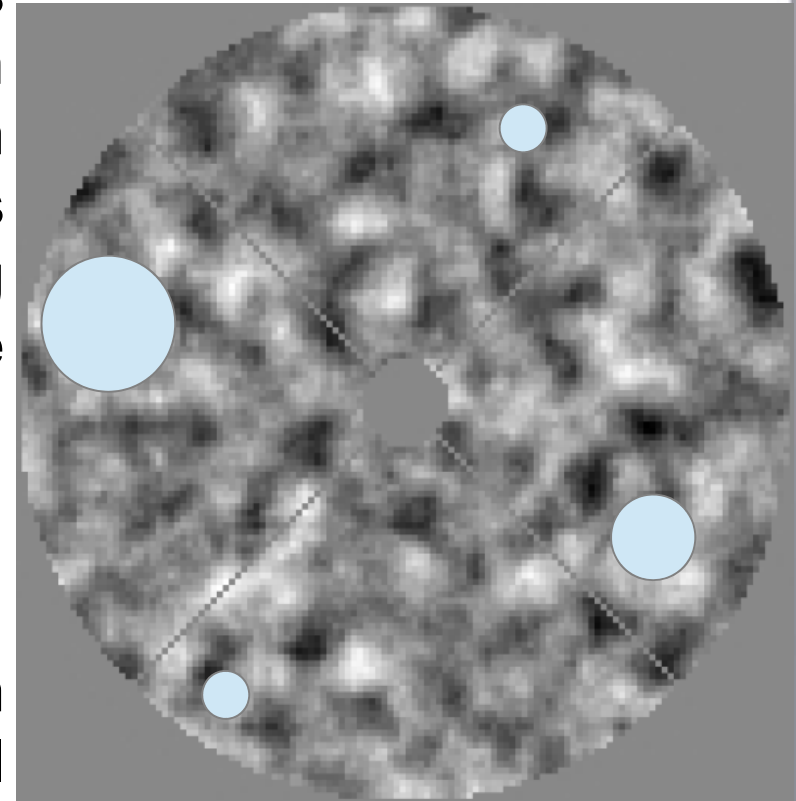
Monthly average of Fried parameter

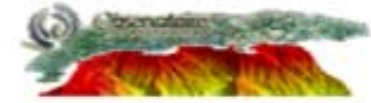
Fried's parameter estimation monthly median values



Pupil plane

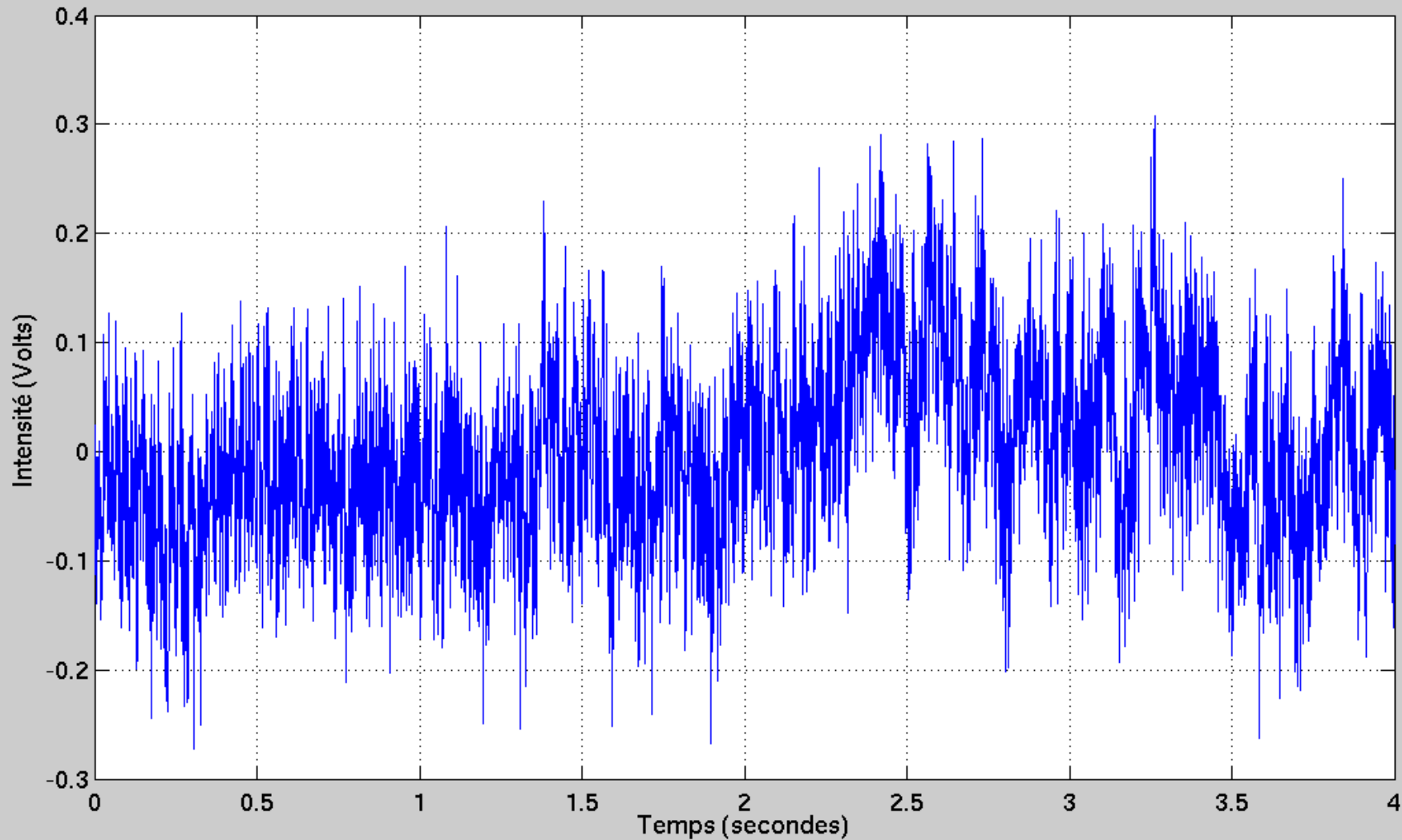
- Telescope pupil is observed by means of a lens through a narrow slit placed on the solar limb image. The diaphragm size is 2" wide and 40" arcseconds length. The pupil image intensity (flying shadows) present fluctuations which are proportional to the AA-fluctuations
- Optical fiber and photodiodes are used
- Low noise amplification
- Temporal structure functions from signals allow to measure temporal characteristic time
- Spatial parameters can be measured by use of a pair of photodiodes

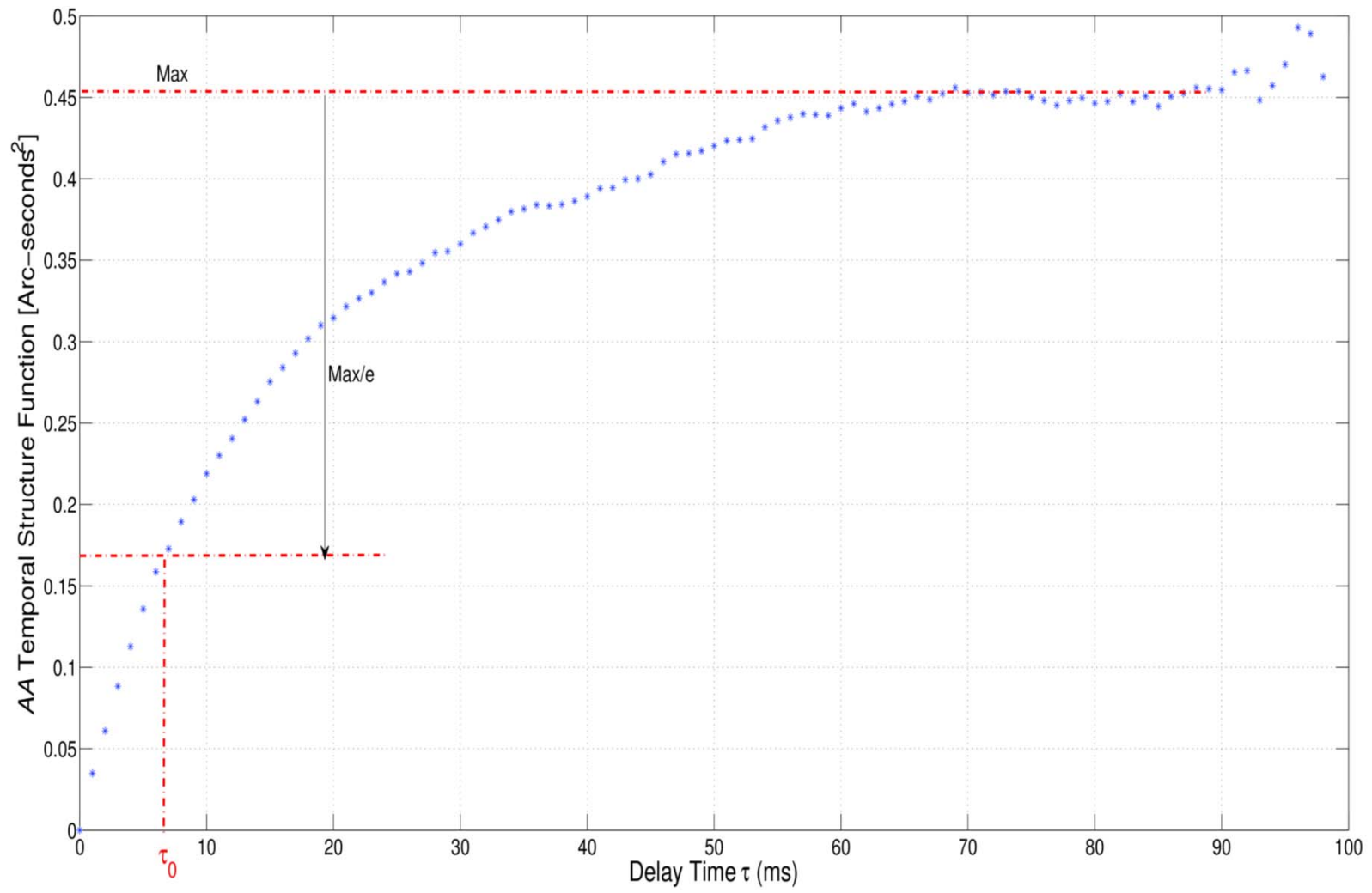
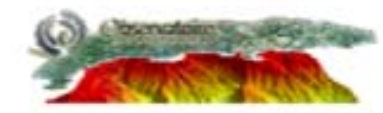




Example signal: fiber 0,5mm

Fluctuation d'intensité voie pupille corrigées de la valeur moyenne





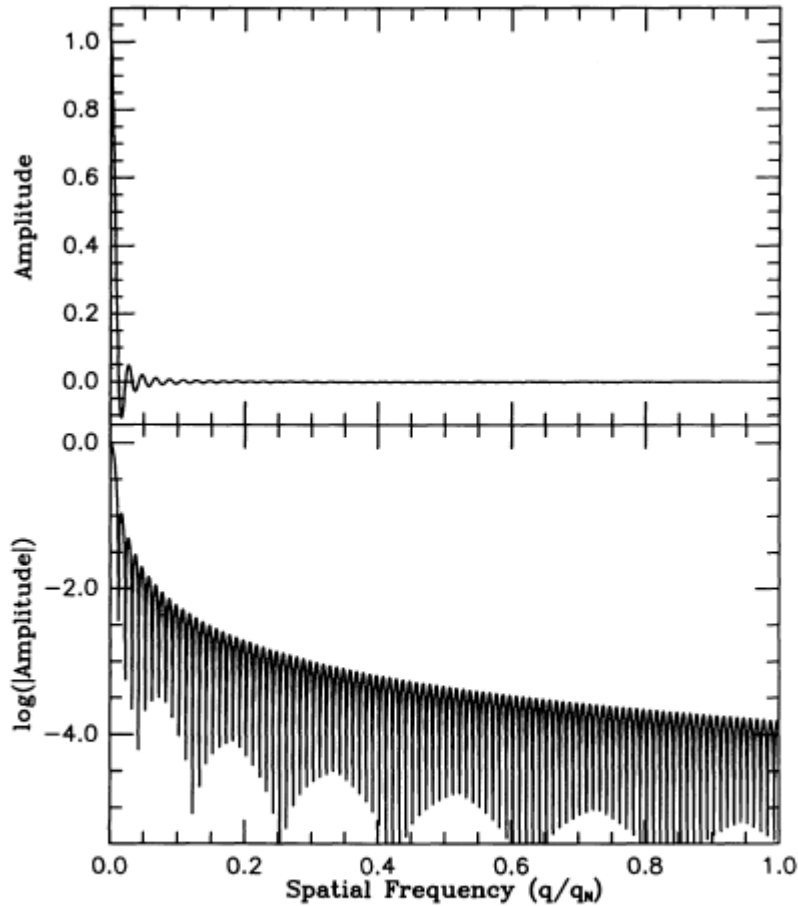
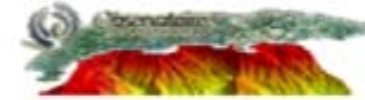


FIG. 1.—An example of the Hankel transform of the limb-darkening function defined by eq. (2) with $N = 2$. The x-axis is the spatial frequency relative to the Nyquist frequency. The upper panel shows the amplitude spectrum, while the lower panel shows the logarithm of its modulus.

$$i(\lambda, r) = \sum_{n=0}^{n=N} a_n(\lambda) \mu^n(r), \quad (2)$$

where

$$\sum_{n=0}^{n=N} a_n(\lambda) = 1,$$

$\mu(r) = [1 - (r/R_T)^2]^{1/2}$ and R_T is the true radius

The hankel transform (def): $F(q) \equiv 2\pi \int_0^\infty f(r) J_0(2\pi r q) dr$

The hankel transform of the limb darkening function:

$$I(q) = \beta R_T \sum_{n=0}^{n=N} \frac{a_n 2^{n/2} \Gamma[(n+2)/2] J_{(n+2)/2}(\beta q)}{(\beta q)^{(n+2)/2}}, \quad (6)$$

where $\beta = 2\pi R_T$, and Γ is the gamma function (Bevington 1969, p. 122).